IOPscience iopscience.iop.org

Home Search Collections Journals About Contact us My IOPscience

Magneto-elastic transition and magnetic couplings: a ^{57}Fe Mössbauer spectroscopy study of the $MnFeP_{1-x}As_x$ system

This article has been downloaded from IOPscience. Please scroll down to see the full text article.

1996 J. Phys.: Condens. Matter 8 8653

(http://iopscience.iop.org/0953-8984/8/44/015)

View the table of contents for this issue, or go to the journal homepage for more

Download details:
IP Address: 171.66.16.207
The article was downloaded on 14/05/2010 at 04:26

Please note that terms and conditions apply.

J. Phys.: Condens. Matter **8** (1996) 8653–8667. Printed in the UK

Magneto-elastic transition and magnetic couplings: a ^{57}Fe Mössbauer spectroscopy study of the $MnFeP_{1-x}As_x$ system

Bernard Malaman†, Gérard Le Caër‡, Pierre Delcroix‡, Daniel Fruchart§, Madeleine Bacmann§ and Robert Fruchart‖

† Laboratoire de Chimie du Solide Minéral, Université Henri Poincaré Nancy I, BP 239, 54506 Vandœuvre les Nancy Cedex, France

‡ Laboratoire de Science et Génie des Matériaux Métalliques, associé au CNRS URA 159, Ecole des Mines, Parc de Saurupt, 54042 Nancy Cedex, France

§ Laboratoire de Cristallographie, CNRS, BP 166, 38042 Grenoble Cedex 9, France

‖ Laboratoire de Matériaux et de Génie Physique, INPG, BP 45, 38402 Saint Martin d'Hères Cedex, France

Received 7 May 1996, in final form 29 July 1996

Abstract. A systematic study of $MnFeP_{1-x}As_x$ ($0.20 \leqslant x \leqslant 0.50$) solid solutions was undertaken by ^{57}Fe Mössbauer spectroscopy. The results confirm previous magnetization and neutron diffraction measurements. In the concentration range $x \geqslant 0.30$, in which the compounds are ferromagnetic, large hyperfine fields agree with the Mn and Fe moment values. In contrast, smaller average fields are measured at low temperature in the antiferromagnetic state ($x \leqslant 0.26$) from broadened Mössbauer spectra. The latter results are consistent both with the reduced value of the Fe moment and with the non-collinearity of the Fe and Mn moments. The magneto-elastic ferromagnetic $\Leftrightarrow$ antiferromagnetic transition has been clearly demonstrated for $x = 0.275$ and $x = 0.30$.

1. Introduction

Crystal structures and magnetic properties of ternary phosphides and arsenides MM′X (M and M′ = transition metals; X = P, As) have already been studied intensively. A few parameters, governing their behaviour with temperature, pressure and the nature of the alloyed elements, have been discussed in [1, 2]. Detailed magnetic studies have been undertaken, particularly by using neutron diffraction [3, 4] and Mössbauer spectroscopy [5–13]. Theoretical predictions of the iron magnetic polarization at different crystal sites have been deduced from electronic structure calculations [7, 8, 14, 15].

More recently our attention was focused on $MnFeP_{1-x}As_x$ solid solutions. In the range of composition $0.15 \leqslant x \leqslant 0.66$ they crystallize with the hexagonal Fe_2P type structure. A magneto-elastic transition was found to be associated with a modification from a ferromagnetic to an antiferromagnetic type of magnetic ordering [16]. This transformation is markedly field-sensitive; it was shown to correspond to changes in the magnetic moments of iron atoms and to modifications in the magnetic exchange couplings [17, 18]. Hereafter we report on detailed investigations undertaken by ^{57}Fe Mössbauer spectroscopy.

0953-8984/96/448653+15$19.50 © 1996 IOP Publishing Ltd

2. Experimental

Powdered samples with $x = 0.20, 0.26, 0.275, 0.30$ and 0.50 were synthesized by heating appropriate mixtures of MnFeP and MnFeAs at 950 °C in evacuated silica tubes for a few days. After 2 days of subsequent treatment at 750 °C, the samples were air-cooled to room temperature. Finally, the samples were checked by x-ray diffraction [16]. In addition, a hexagonal FeMnAs sample was prepared under high pressure (30 kbar).

^{57}Fe Mössbauer spectra were recorded between 80 K and room temperature in transmission geometry using a constant-acceleration-mode spectrometer. A ^{57}Co source embedded in a Rh matrix, with a strength of $\approx$ 15 mCi was used. The iron Mössbauer spectra were analysed either by using a least-squares fitting program assuming Lorentzian peaks or by using a method that considers hyperfine field distributions $P(H)$ for the experimental spectra [19]. As is usually done, the ^{57}Fe isomer shifts are relative to α-Fe at room temperature and peaks of a given sextuplet are labelled from 1 to 6, from negative to positive velocities respectively.

3. Crystal and magnetic structures

The $MnFeP_{1-x}As_x$ compounds with $0.15 \leqslant x \leqslant 0.66$ crystallize with the Fe_2P-type structure (space group $P62m$). No preferential atom ordering between P and As on the 1(b) and 2(c) sites is observed. Iron atoms are almost exclusively located in the 3(f) tetrahedral sites (namely with coordination number CN(P, As) = 4) and manganese atoms in the 3(g) pyramidal sites (CN(P, As) = 5). A very slight deviation ($\leqslant$ 6%) from complete metal ordering is detected [17]. The x dependences of cell parameters and of reduced atomic coordinates are reported in the latter reference.

The magnetic phase diagram of the $MnFeP_{1-x}As_x$ system is represented in figure 1 [16]. Three types of magnetic transitions are observed according to x: ferro–paramagnetic for $\approx 0.30 \leqslant x \leqslant 0.66$, antiferro–paramagnetic for $\approx 0.15 \leqslant x \leqslant \approx 0.26$ and ferro–antiferromagnetic transition followed by an antiferro–paramagnetic transition for $\approx 0.26 \leqslant x \leqslant \approx 0.30$.

The aforementioned magnetic structures have been determined by neutron diffraction [17]. In the ferromagnetic state, the easy axis lies in the $(\boldsymbol{a}, \boldsymbol{c})$ plane. For the $x = 0.5$ sample, the moments are all directed along the $\boldsymbol{c}$ axis whereas, for the $x = 0.3$ compound, the moment direction deviates from the $\boldsymbol{c}$ axis by $\beta \approx 50^\circ$. In both samples the saturation moments are $\mu(\text{Mn}) \approx 2.6\mu_B$ and $\mu(\text{Fe}) \approx 1.2\mu_B$. The antiferromagnetic long-period ordering ($\boldsymbol{Q} = (0, q_y, 0)$) is characterized by a helical configuration of the Mn moments within the $(\boldsymbol{a}, \boldsymbol{c})$ plane. The Fe moments are directed along the $\boldsymbol{c}$ direction, oscillating in amplitude along the propagation direction $\boldsymbol{b}^*$. At $T = 1.45$ K, the Mn moment is $2.4\mu_B$, $q_y = 0.35$ and the maximum value of the sinusoidal amplitude of the Fe moment is $0.45\mu_B$ for $MnFeP_{0.80}As_{0.20}$. Figure 2 shows schematized representations of the long-range magnetic structure for $q_y = \frac{1}{3}$.

4. The paramagnetic state

At 295 K, Mössbauer spectra of the $MnFeP_{1-x}As_x$ hexagonal solid solution ($0.2 \leqslant x \leqslant 0.5$) consist mainly in an intense but slightly broadened absorption line (figure 3). A similar 'one-line'-like spectrum is also observed for orthorhombic MnFeP and hexagonal MnFeAs compounds. Moreover, a very weak extra line is also seen for all samples on the positive

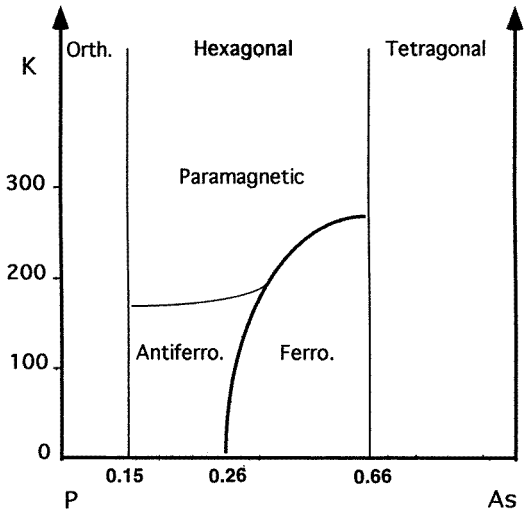

Figure 1. The magnetic phase diagram of the $MnFeP_{1-x}As_x$ system.

side of the velocity scale. According to the neutron diffraction study (section 3), the two sets of lines can be attributed without ambiguity to the tetrahedral site for the main spectral component and to the pyramidal site for the weak one. On average, $\approx 5\%$ of the pyramidal sites are occupied by Fe atoms. Because this latter component is too weak to be calculated safely, we will not discuss its hyperfine parameters further. Only slight changes of the isomer shift δ and of the quadrupole splitting Δ occur when x (the As concentration) increases. For the tetrahedral site, $\delta_t = 0.33 \pm 0.02$ mm s^{-1} when $0.20 \leqslant x \leqslant 0.30$ (0.39 ± 0.01 mm s^{-1} for $x = 0.50$) and $\Delta_t = 0.16 \pm 0.01$ mm s^{-1}. Although clear differences exist between hyperfine parameters of ^{57}Fe in tetrahedral sites in various compounds with orthorhombic, hexagonal or tetragonal structures, general features such as similar and small Δ_t values (table 1) are maintained. It is worth mentioning that the main central doublet in metastable hexagonal FeMnAs, associated with the tetrahedral site, yields $\delta_t = 0.47 \pm 0.02$ mm s^{-1} and $\Delta_t = 0.18 \pm 0.01$ mm s^{-1}. Weaker lines (figure 3) on the low-velocity side are associated with tetragonal FeMnAs, the equilibrium form at ambient pressure.

Table 1. Comparison of quadrupole splittings of ^{57}Fe in tetrahedral sites of various compounds.

Compounds	Δ_t (mm s^{-1})	References
Hexagonal Fe_2P	0.10(1)	[4]
Tetragonal Fe_2As	0.13(1)	[13]
Hexagonal FeMnAs	0.18(1)	This work
Hexagonal $MnFeP_{1-x}As_x$	0.16(1)	This work

We conclude that the almost perfect occupancy of tetrahedral sites ($\approx 95\%$) deduced from Mössbauer spectra agrees with diffraction results and with the general rules previously established for such compounds [1]. Moreover, the small Δ_t values will allow us to simplify the analyses of Mössbauer spectra recorded in the magnetic state by justifying the use of

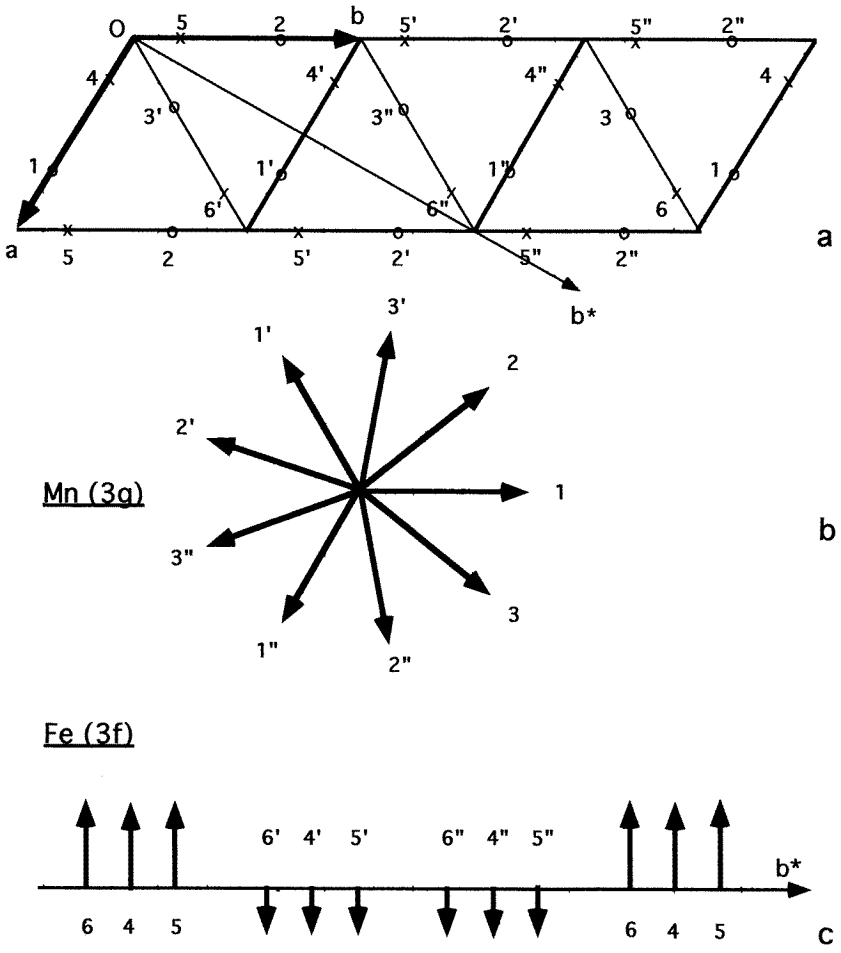

Figure 2. A schematic representation of the antiferromagnetic structure of $MnFeP_{0.8}As_{0.2}$ for $q_y = \frac{1}{3}$ (see the text): (a) Mn (open circles) and Fe (crosses) atomic positions in the magnetic cell $(a, 3b, c)$, (b) a representation at a common origin of Mn moments in the $(\boldsymbol{a}, \boldsymbol{c})$ plane (c) a representation along the $\boldsymbol{b}^*$ direction of the Fe moments. The moments are parallel to the $\boldsymbol{c}$ axis. Because $q_y = \frac{1}{3}$, the largest moment values $(4, 5, 6)$ are twice the smallest ones $(4', 5', 6', 4'', 5'', 6'')$.

first-order perturbation theory: $\Delta \ll |g_{3/2}H|$, where H is the hyperfine field and $g_{3/2}$ the nuclear g factor for the excited state.

5. The ferromagnetic state

The compounds with $x = 0.275, 0.3$ and 0.5 are ferromagnetic (F) at 80 K yielding Mössbauer spectra composed of six broadened lines (figure 4(a)). Line broadening decreases from outer to inner lines: $\Gamma_{1,6} = 0.58$ mm s^{-1}, $\Gamma_{2,5} = 0.45$ mm s^{-1} and $\Gamma_{3,4} = 0.36$ mm s^{-1}. There exists thus a distribution of sextuplets which is not expected on the basis of the ferromagnetic structure. However, there is a distribution of As and P

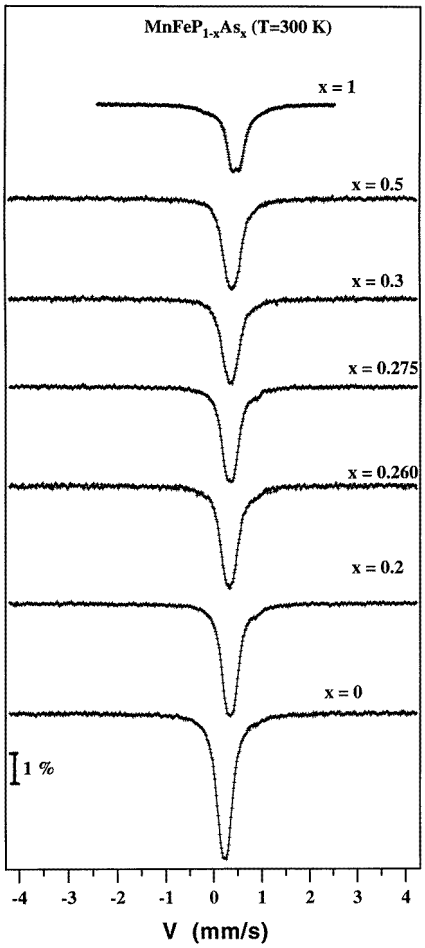

Figure 3. ^{57}Fe room-temperature Mössbauer spectra of orthorhombic FeMnP, of hexagonal $MnFeP_{1-x}As_x$ solid solutions ($x = 0.2$, 0.26, 0.275, 0.3 and 0.5) and of hexagonal MnFeAs metastable at ambient pressure.

environments for Fe_t atoms. Assuming a random distribution of As and P on the metalloid sites, we obtain the probability $p(n)$ for an iron atom to have n As and $(4-n)$ P neighbours:

$$p(n) = C_4^n x^n (1-x)^{4-n}. \tag{1}$$

Table 2 gives a comparison between the calculated values of $p(n)$ (equation (1)) and the fitted values for $x = 0.5$. The agreement is fair. Because the line broadening is not too strong, however, we found it more interesting and reliable to fit the spectra also by constraining the intensities of the five sub-spectra according to equation (1). A reasonable and consistent picture emerges from such calculations.

(i) The isomer shifts are approximately the same for all sites with a maximum difference less than ≈ 0.03 mm s^{-1}. The average isomer shifts are 0.48(2), 0.48(2) and 0.51(2) mm s^{-1} for $x = 0.275, 0.3$ and 0.5 respectively.

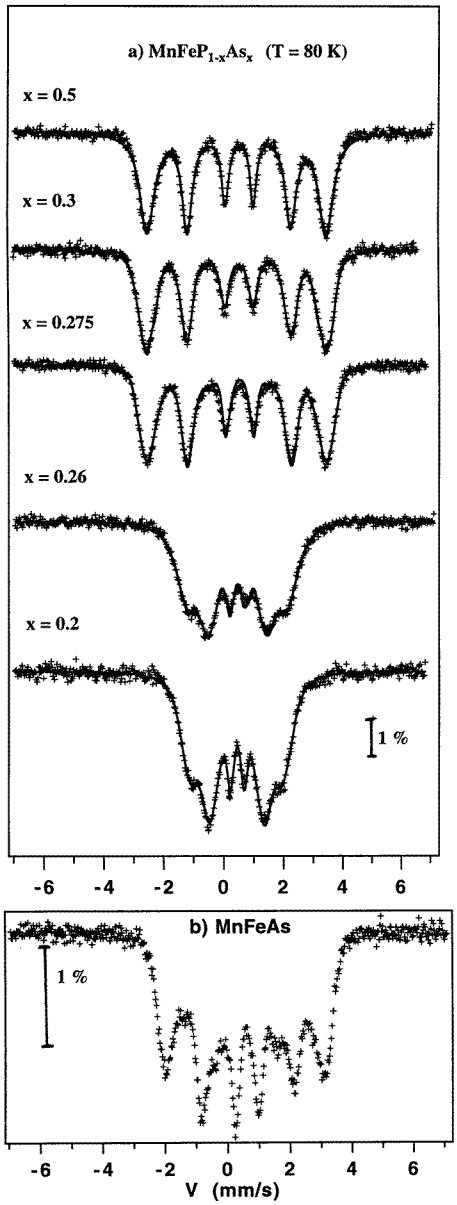

Figure 4. ^{57}Fe Mössbauer spectra at 80 K of (a) hexagonal $MnFeP_{1-x}As_x$ solid solutions ($x = 0.2$, 0.26, 0.275, 0.3 and 0.5) and (b) high-pressure hexagonal MnFeAs.

(ii) Whatever the fitting conditions (one sextuplet, five sextuplets or a hyperfine field distribution), a non-zero quadrupolar shift 2ε, almost identical for all sub-spectra, is found from line positions V_i to be

$$2\varepsilon = [(V_6 - V_5) - (V_2 - V_1)]/2 = -0.08(2) \text{ mm s}^{-1}.$$

(iii) The five fields are observed to be regularly spaced with a step of about ≈ 14 kG (table 2). The mean field $\langle H \rangle_F$ is about 185(1) kG at 80 K.

Table 2. Mössbauer parameters at $T = 80$ K for $MnFeP_{0.5}As_{0.5}$.

n	Non-metal neighbourhood of Fe	Calculated $p(n)$	Intensity	H (kG)	H (kG) constrained fit
4	0P, 4As	0.0625	0.09	150	150
3	1P, 3As	0.25	0.21	170	172
2	2P, 2As	0.375	0.34	184	186
1	3P, 1As	0.25	0.22	195	199
0	4P, 0As	0.0625	0.13	207	212

Because the point symmetry at the tetrahedral iron site is mm, one of the principal axes of the electric field gradient (EFG) tensor is parallel to the $\boldsymbol{c}$ axis while a second axis is parallel to the $\boldsymbol{a}$ axis, the third one being obviously perpendicular both to $\boldsymbol{a}$ and to $\boldsymbol{c}$. It is not known *a priori* which one is the V_{zz} axis and neither is the value of the asymmetry parameter η known. According to Wäppling *et al* [6], η would be of the order of 0.1–0.3 for Fe_2P. The quadrupole splitting (Δ) is known to be almost constant when temperature decreases below room temperature in such compounds. It is even approximately constant in the range 0–800 K for Fe_t in Fe_2P [6]. When first-order perturbation holds, the quadrupolar shift (2ε) is related to the electric field gradient V_{ZZ} by

$$2\varepsilon = [(eQV_{ZZ})/2][3\cos^2\theta - 1 + \eta\sin^2\theta\cos(2\phi)] \tag{2}$$

where Q is the nuclear quadrupole moment of the excited state. In the paramagnetic state only the quadrupole splitting Δ, given by

$$\Delta = \left|\frac{eQV_{ZZ}}{2}\right|(1+\eta^2/3)^{1/2}$$

is measured.

In the present case, the first-order expression (equation (2)) is valid because $\Delta(= 0.16\ \text{mm s}^{-1}) \ll |g_{3/2}\langle H\rangle_F|(= 1.25\ \text{mm s}^{-1})$. The angles θ and ϕ are the polar angles of the hyperfine field direction in the frame of the EFG tensor principal axes. The magnetic moments are known to be parallel to the $\boldsymbol{c}$ axis for $x = 0.50$. The angle θ is thus either 0 or 90°. For $\theta = 0$, we should observe $2\varepsilon = 0.16(1)\ \text{mm s}^{-1}$ (section 4) instead of the measured value $-0.08(2)\ \text{mm s}^{-1}$. The angle θ is therefore 90°, that is V_{zz} lies in the basal plane and $2\varepsilon \approx 0.16(-0.5 + 0.5\eta\cos(2\phi))$. Because ϕ is either 0 or 90°, we conclude that η is close to zero, as it is in Fe_2P for the same type of Fe site. Finally, the values of 2ε are almost identical for $x = 0.30$ and 0.50. A deviation of the easy direction from the $\boldsymbol{c}$ axis as large as 50° [17] thus seems difficult to reconcile with the value $2\varepsilon = -0.08\ \text{mm s}^{-1}$. Moreover, according to the hexagonal symmetry of the unit cell, there exist three different frames of EFG principal axes which would yield three different values of 2ε for collinear fields. The angle θ is about 90° for all Fe atoms only if the spin direction is close to the direction of the $\boldsymbol{c}$ axis.

The effect of the As for P substitution on the Fe hyperfine field can be deduced from the concentration-dependence of the intensities of the various sub-spectra. Before discussing that point, it is worthwhile mentioning that the contribution of Fe atoms on pyramidal sites ($Fe_p \approx 5\%$, section 4) cannot be reliably retrieved from the experimental broadened spectra. Moreover, the Fe_p contribution is probably also split into six sub-spectra related to the distribution of non-metal environments around Fe_p atoms (n As, $(5-n)$ P, $n = 0, \ldots, 5$). The pyramidal contribution is therefore neglected in the present discussion because the global understanding comes from sites which have a relative weight much larger than 5%.

For $x = 0.275$ and 0.30, only four sub-spectra contribute significantly to the total spectrum as $p(4) < 0.01$. For $x = 0.50$, the most intense sextuplet is consistently attributed to a (2As, 2P) environment of Fe_t atoms. The fact that a component with a field of 150 kG is no longer observed for $x = 0.30$ suggests that one should attribute that field to a (4As, 0P) metalloid environment of Fe_t atoms. In ferromagnetic hexagonal MnFeAs (figure 4(b)) the most probable field $H = 158$ kG seems to reinforce the latter assumption. It would be desirable to show further that the iron magnetic moments are comparable in the two structures. It seems, however, reasonable to conclude that the hyperfine field decreases with the number n of As neighbours of Fe_t atoms. If we further assume that the field H(nAs, $(4-n)$P) $= H(n)$ is given by:

$$H(n) = H(0) - n\Delta H \tag{3}$$

then we deduce from equations (1) and (3) that the mean field is $\langle H\rangle_F = H(0) - 4x\Delta H$, whereas the standard deviation is $\sigma_H = |\Delta H|[4x(1-x)]^{1/2}$. The values of $\langle H\rangle_F$ and of σ_H obtained from fittings of spectra for $x = 0.275, 0.3$ and 0.5 yield $\Delta H = 14(1)$ kG and $H(0) = 210(8)$ kG.

The field $H(0)$ would therefore be much larger than the field of Fe_t atoms surrounded by four phosphorus atoms in hexagonal Fe_2P: $H(0) = 109(1)$ kG at 80 K [6]. To know the origin of such a difference, we notice that the Fe_t magnetic moment is close to $1\mu_B$ at 80 K in Fe_2P whereas it is $1.48\mu_B$ at 200 K in $FeMnP_{0.5}As_{0.5}$ [17]. Moreover, a Mn moment of $2.02\mu_B$ has also been measured in the latter compound [17]. To estimate a value of the Fe moment either from $\langle H\rangle_F$ or from $H(0)$, we use a factor of proportionality 142 kG/μ_B deduced by Eriksson and Svane [14] from a thorough theoretical investigation of magnetic hyperfine fields in various compounds. The hyperfine field of Fe_t in Fe_2P follows the general trend [14]. In contrast, the hyperfine field of Fe_p deviates significantly from the overall linear relation [14]. That anomalous behaviour originates from the polarization of the iron 4s valence electrons which are polarized parallel rather than antiparallel to the iron d moment [14]. Severin *et al* [8] used the latter model successfully in $Fe_2P_{1-x}Si_x$. The iron moment is deduced to be $1.3\mu_B$ and $1.5\mu_B$ from $\langle H\rangle_F$ and $H(0)$ respectively. The excellent agreement with the neutron diffraction value [17], $\mu_{Fe} = 1.48\mu_B$, may be partly fortuitous insofar as we have ignored the fact that the larger Mn moment, $\mu_{Mn} = 2.02\mu_B$ [17], also gives a contribution to the total field. A semi-empirical model which includes such moments will be discussed in section 6.

In conclusion, the relative field change $\Delta H/\langle H\rangle_F \cong 0.07$ is quite comparable to the change (≈ 0.07) of iron fields in Fe-rich alloys with a variety of elements. Its magnitude $\Delta H = 14$ kG, which is much less than ΔH(Fe alloys) ≈ 23 kG, renders the spectra more difficult to fit. In spite of such difficulties, a consistent picture emerges: the replacement of a P atom by an As atom decreases the field of their Fe_t neighbours by about 14 kG. The average field of Fe_t atoms in the ferromagnetic state is 185 kG at 80 K. An extrapolated value of 200 kG at 0 K is obtained from experiments described in the next section. The much larger value of H for Fe_t atoms in hexagonal $FeMnP_{1-x}As_x$ compared with H in hexagonal Fe_2P is related to the enhanced Fe_t moment and to the large Mn moment (see also section 6).

6. The antiferromagnetic state

Mössbauer spectra have been recorded at 80 K for $x = 0.20$ and 0.26 (figure 4(a)). The ferromagnetic–antiferromagnetic transition which occurs for $x = 0.275$ and 0.30 at $T \geqslant 130$ and $\geqslant 170$ K respectively (figure 1) has also been investigated. Figure 4(a) shows strong

differences between Mössbauer spectra of ferromagnetic (F) and antiferromagnetic (AF) $FeMnP_{1-x}As_x$ at 80 K. A magnetic hyperfine field distribution (HFD) with a strongly reduced mean field compared with the field value in the ferromagnetic state is clearly visible. Figure 5 shows two typical HFDs at 80 K calculated with a constrained Hesse–Rübastsch method [19] both in F and in AF states. A slight asymmetry of the AF spectra was accounted for in terms of a linear relation between the isomer shift δ and the field H with a slope of 9×10^{-4} kG mm^{-1} s. Good fits can be obtained only for a zero quadrupolar shift (2ε). As detailed in section 5, the pyramidal contribution hidden within the broad hyperfine field distribution has been neglected.

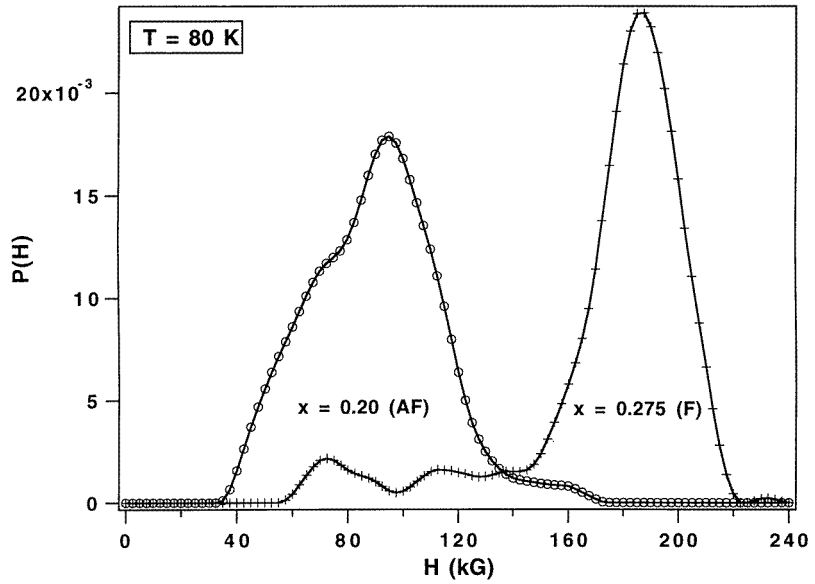

Figure 5. Magnetic hyperfine field distributions calculated from ^{57}Fe Mössbauer spectra at 80 K of the ferromagnetic $MnFeP_{0.725}As_{0.275}$ and of the antiferromagnetic $MnFeP_{0.80}As_{0.20}$.

The average hyperfine field is $\langle H \rangle_{AF} = 90(1)$ kG and the standard deviation is $\sigma_H = \langle (H - \langle H \rangle_{AF})^2 \rangle^{1/2} = 28(1)$ kG whereas $P(H)$ is maximum for $H = 95$ kG. The mean field in the AF state is therefore half that in the F state at $T \leqslant 80$ K (figure 5). The decrease in the Fe moment alone cannot explain the latter result: the mean field $\langle H \rangle_{AF}$ is not proportional to the iron moment alone with a reasonable value of the proportionality constant, as for the F state (≈ 146 kG/μ_B). In the incommensurate AF state, the Fe moment μ_{AF} is directed along the $\boldsymbol{c}$ axis and it oscillates in amplitude (see figure 2) [17]. A Fe field $H_{AF} = A\mu_{AF}$ with $\mu_{AF} = \mu_0 \sin\theta$ would yield [20] the following.

(i) A hyperfine field distribution $P(H) \propto (H_0^2 - H^2)^{-1/2}$ with $H_0 = A\mu_0$, with a mean field $\langle H_{AF} \rangle = 2H_0/\pi$ and $\sigma_H = H_0(\frac{1}{2} - 4/\pi^2)^{1/2}$, that is $\sigma_H/\langle H_{AF} \rangle \approx 0.48$,

(ii) a quadrupolar shift $2\varepsilon = -0.08$ mm s^{-1} because $\theta = 90^\circ$ (see section 4) whatever the field.

None of these conclusions agree with experiment: $\sigma_H/\langle H_{AF} \rangle$is 0.31 (2) and $\varepsilon = 0$. The mean field $\langle H_{AF} \rangle$ would moreover be 42 kG, for $A = 146$ kG/μ_B and $\mu_0 = 0.45\mu_B$ [17], instead of 90 kG.

There are two main reasons for such discrepancies:

(i) the Mn magnetic moments are not collinear with the Fe magnetic moments [17] (figure 2) and

(ii) $\mu_{Mn} = 2.4\mu_B$ is much larger than μ_{Fe} [17].

A semi-empirical model which has been successfully applied to various intermetallic or semi-metallic compounds will be used to account for the observed HFD. The hyperfine field $\boldsymbol{H}$ will be assumed to be the vector sum of contributions [21] which are

(i) collinear with the moment of the iron atom itself $\mu_{Fe(0)}$ and

(ii) collinear with the moments of its first Mn and Fe neighbours: two Fe_t at 2.67 Å ($\mu_{Fe(1)}$), two Mn_p at 2.69 Å($\mu_{Mn(1)}$) and four Mn_p at 2.81 Å($\mu_{Mn(2)}$), with the associated proportionality constants a, b_1, c_1 and c_2 respectively:

$$\boldsymbol{H}_{AF} = a\mu_{Fe(0)} + 2b_1\mu_{Fe(1)} + 2c_1\mu_{Mn(1)} + 4c_2\mu_{Mn(2)}. \tag{4}$$

To simplify the calculation, we consider the commensurate AF structure with a propagation vector $\boldsymbol{Q} = [0, q_y, 0]$ [17] with $q_y = \frac{1}{3}$, the value which is obtained for $x = 0.20$ (figure 2). Three different μ_{Fe} vectors are found in such an AF structure: one equal to $\mu_{Fe} = 0.45\boldsymbol{k}$ and two equal to $-0.225\boldsymbol{k}$, where $\boldsymbol{k}$ is a unit vector parallel to $\boldsymbol{c}$.

The Mn moments are arranged in an helical configuration which propagates in a direction perpendicular to the $(\boldsymbol{a}, \boldsymbol{c})$ plane. Because they are not collinear to the Fe moments, the total fields make different angles with the V_{zz} axis of the corresponding Fe atoms. That explains the averaging of the quadrupolar shift ε to 0. When all possible configurations are taken into account, a field distribution with five peaks is obtained. In all cases $\mu_{Fe(1)} = \mu_{Fe(0)}$ and the respective weightings of the five fields are $\frac{2}{9}$ except for one field, for which the weighting is $\frac{1}{9}$. Finally, the latter field distribution is convoluted with a Gauss distribution of standard deviation σ to represent the effect of the distribution of As–P environments of every Fe atom. The value $\sigma = 14$ kG has been obtained from good fits of the Mössbauer spectra with hyperfine field distributions in the ferromagnetic state at 80 K (figure 5). The HFDs so obtained are indeed very close to Gauss distributions. The final step consists of comparing the HFD calculated in that way to the experimental HFD for $x = 0.2$ at 80 K. At most, three parameters $A = a + 2b_1, c_1$ and c_2 may be varied.

Figure 6 shows the best agreement obtained with the assumption $c_1 = c_2$. Some features of the experimental distribution are correctly reproduced. A much better agreement is obtained for $c_1 > c_2$ (figure 6). The parameters c_1 and c_2 are not very sensitive to the value of A which may be taken here as $A = 52(10)$ kG/μ_B with $c_1 = 10.6(2)$ kG/μ_B and $c_2 = 6.0(5)$. If such constants are used, fields of 133 and 178 kG are calculated at 80 K for ferromagnetic Fe_2P ($\mu_{Fet} = 0.98\mu_B$, $\mu_{Fep} = 1.82\mu_B$) as derived from [5] and for ferromagnetic $FeMnP_{0.7}As_{0.3}$ ($\mu_{Fe} = 1\mu_B$, $\mu_{Mn} = 2.8\mu_B$ at 100 K [17]), respectively. The calculated fields are in very reasonable agreement with the observed ones namely 109 and 180 kG, respectively. It seems difficult to relate the various contributions of the semi-empirical model used here to the more global contributions calculated in theoretical electronic structure calculations. Moreover, the semi-empirical model used in this section is made simpler when chosing $q_y = \frac{1}{3}$, that is exactly the value corresponding to the studied compositions. We nevertheless expect b_1 to be of the opposite sign of a (4) whose magnitude is known to be much larger than 50 kG/μ_B. In any case, hyperfine fields which are not collinear with the Fe moments are clearly needed to explain the experimental results. That conclusion may be helpful for eventual future theoretical calculations in such hexagonal solid solutions. The results of Mössbauer spectroscopy are thus completely consistent with neutron diffraction conclusions about the non-collinear AF structure and the strong reduction of the Fe moment in the AF state compared with the F state.

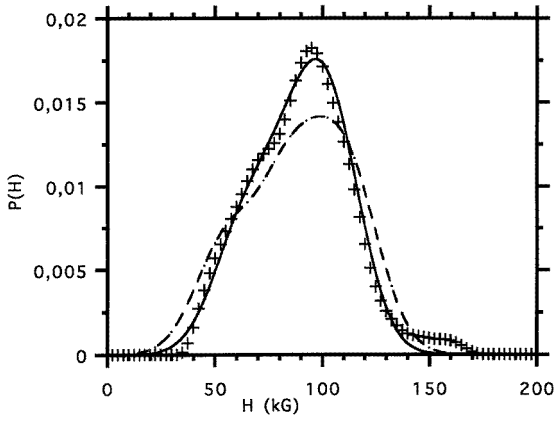

Figure 6. A comparison between the experimental hyperfine field distribution (crosses) in the antiferromagnetic $MnFeP_{0.80}As_{0.20}$ at 80 K and the distributions calculated with the model described in section 6 (equation (4)): $A = a + 2b_1 = 52.5$ kG, $c_1 = c_2 = 7.5$ kG and $\sigma = 14$ kG (chain line) and $A = 52.5$ kG, $c_1 = 10.6$ kG, $c_2 = 6$ kG, $\sigma = 14$ kG (full line).

7. A study of the magneto-elastic transition

Mössbauer spectra have been recorded for $x = 0.275$ and for 0.30 in temperature ranges in which the magneto-elastic F $\rightarrow$ AF transition occurs [16, 17] (see also figure 1). The latter transition is clearly observed in both cases (figure 7). Mössbauer spectra have been calculated with hyperfine field distributions. The characteristics found for every magnetic phase which are described in sections 5 and 6 were taken into account in the fitting method. Very good fits are obtained on the whole. Figure 7 shows that there exists a temperature range within which F and AF phases coexist. From the $P(H)$ distributions, it is possible to calculate the temperature-dependence of the fraction α_F of iron atoms in the ferromagnetic phase (figure 8) and to draw the following conclusions.

(i) The pure AF domains have widths of about 20 K . The AF domain starts at 160 K for $x = 0.275$ ($T_N = 192(1)$ K) and at 180 K for $x = 0.30$($T_N = 196(1)$ K). Such a composition-dependence agrees with the magnetic measurement results [16] (see also figure 1).

(ii) F and AF phases coexist between about 140 and 160 K for $x = 0.275$ and between about 165 and 180 K for $x = 0.3$. The lower limits of the coexistence domain have been estimated from linear fits to the $\alpha_F(T)$ curves in the temperature range within which it changes abruptly (figure 8). We cannot exclude that small amounts of the AF phase still contribute to the Mössbauer spectra at lower temperatures.

Figure 9 shows the hyperfine fields as a function of temperature in $MnFeP_{0.725}As_{0.275}$. The F–AF transition and the F–AF coexistence domain are clearly seen. The extrapolation of $\langle H \rangle_F$ to $T = 0$ K gives a field of 200(2) kG for both $x = 0.275$ and 0.30.

The question of the very existence of such a mixed domain is relevant. In a system which would show an abrupt transition between the F and AF states, a smooth transition would be observed as a result of temperature fluctuations during the recording of Mössbauer spectra. In the presence of Gaussian fluctuations of width ΔT, a transition width of at most $4\Delta T$ is expected. The reported widths of about 20 K are much too large to be accounted for by temperature fluctuations of at worst $\Delta T = 2$ K. We conclude that F and AF regions

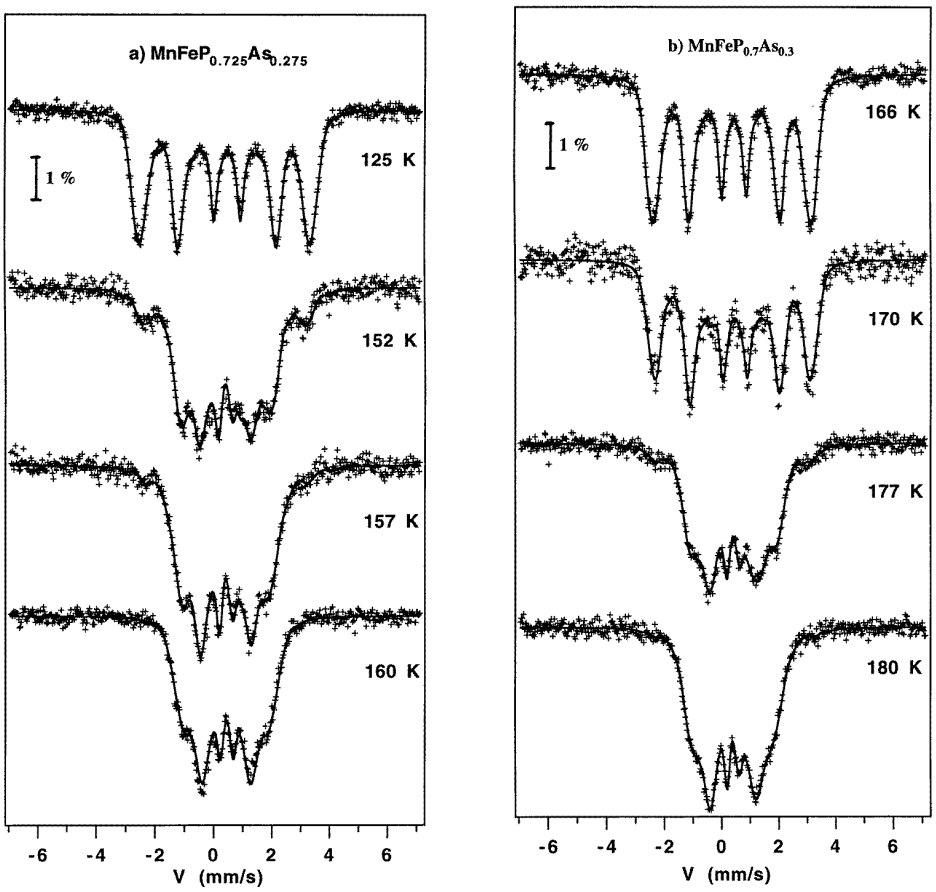

Figure 7. Temperature-dependences of ^{57}Fe Mössbauer spectra of hexagonal $MnFeP_{1-x}As_x$ in the range of the ferromagnetic–antiferromagnetic transition: (a) $x = 0.275$ and (b) $x = 0.30$.

actually coexist in the samples investigated here. Because the AF–F transition temperature strongly depends on concentration, small concentration fluctuations may account for the observed coexistence domain.

8. Discussion and conclusion

^{57}Fe Mössbauer spectra of hexagonal $MnFeP_{1-x}As_x$ ($0.20 \leqslant x \leqslant 0.50$) are in fairly good agreement with magnetization and neutron diffraction measurements. Mössbauer spectra in the paramagnetic state confirm that Fe atoms are located almost exclusively at the tetrahedral sites. As expected from previous magnetic studies, three different types of magnetic transition are observed when the As content increases: AF $\rightarrow$ paramagnetic (P), F $\rightarrow$ AF $\rightarrow$ P and F $\rightarrow$ P.

In the ferromagnetic range ($x \geqslant 0.30$), large average hyperfine fields (200 kG at 0 K) agree well with the Mn and Fe moment values deduced from neutron diffraction data. The hyperfine field direction, which is found to be parallel to the $\boldsymbol{c}$ axis whatever x is, shows,

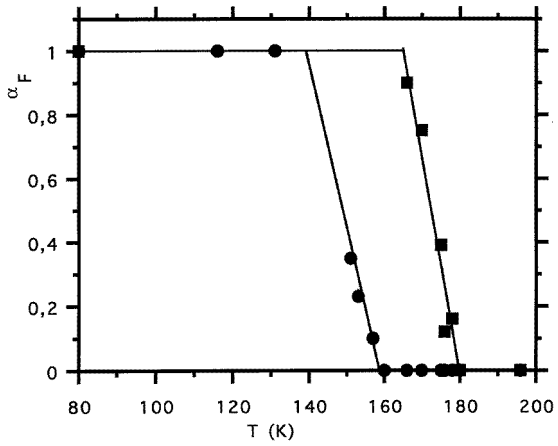

Figure 8. The temperature dependence of the fraction α_F of iron atoms in the ferromagnetic state of $MnFeP_{0.70}As_{0.30}$ (full squares) and of $MnFeP_{0.725}As_{0.275}$ (full circles).

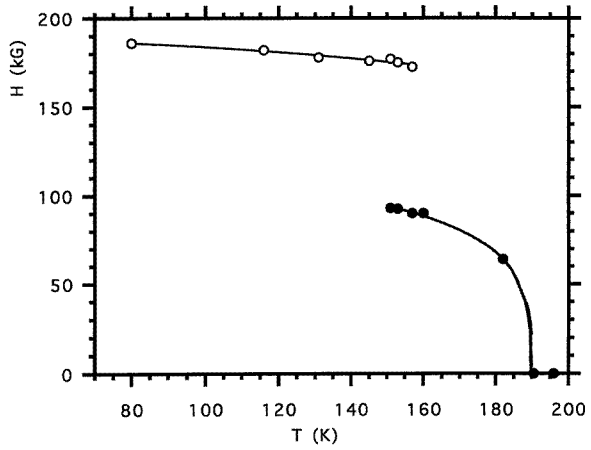

Figure 9. The temperature dependence of the iron hyperfine field both in the ferromagnetic (empty circles) and in the antiferromagnetic (full circles) states of $MnFeP_{0.725}As_{0.275}$.

however, that the moment direction does not tilt from the $\boldsymbol{c}$ axis by about 50° as deduced from the neutron study. Moreover, the substitution of one P neighbour of an Fe atom by an As atom decreases the Fe hyperfine field by about 14 kG at 80 K. A complementary neutron diffraction study of hexagonal MnFeAs is in progress.

In contrast, smaller average hyperfine fields (about 90 kG at 80 K) are measured in the antiferromagnetic state ($x \leqslant 0.26$). Moreover, only hyperfine field distributions can explain the broadening of Mössbauer spectra. A model which considers solely the contribution of the collinear Fe moments fails to account for the observed fields: the non-collinear Mn moments contribute to the Fe hyperfine fields. Thus, the Mössbauer characteristics agree with the reduced value of the Fe magnetic moment and with the non-collinearity of the Fe and Mn moments deduced from the magnetic structure.

The magneto-elastic transition has been clearly demonstrated for $x = 0.275$ and 0.30. In both samples, F and AF regions coexist in a temperature range of about 20 K above 140 and 165 K respectively. Due to the strong dependence of the F $\rightarrow$ AF transition temperature on x, this coexistence of phases may be explained in terms of small fluctuations of concentration in the studied samples. Above 160 and 180 K, only an AF structure is observed up to $T_N = 192$ and 196 K for $x = 0.275$ and 0.30 respectively.

In this series, iron is well suited as a probe to check local magnetic and electronic characteristics of the d band. Manganese almost exclusively occupies pyramidal sites. In contrast, iron atom occupies the tetrahedral ones, which appear the most 'sensitive' site in terms of metal-to-metal distances. A perfectly random As to P substitution with x was found in the $MnFeP_{1-x}As_x$ solid solution. So, no preferential M–X bond (M = Mn, Fe; X = P, As) is formed. In such terms, bearing their iso-electronic p states in mind, the observed transformations are, to a first approximation, only volume-dependent. Hence, the substitution of a P atom by an As atom corresponds to a 'chemical pressure effect' with a net decrease in the hyperfine field (14 kG) of the iron atoms in the tetrahedral site.

In a previous paper [17], it was found that, in the $MnFeP_{1-x}As_x$ series, Fe–Fe and Mn–Fe distances change abruptly at the AF/F transition which occurs as a function of x and T in the way shown by figure 1 (see also section 7). These variations affect principally the Fe–Fe nearest neighbours distances and the two shortest Mn–Fe distances which exhibit an increase and a decrease of $\approx 4\%$ at the AF $\rightarrow$ F transition, respectively. The Fe–Fe distances are ≈ 2.64 and 2.72 Å whereas the Mn–Fe distances are ≈ 2.67 and 2.58 Å, in the AF and F states, respectively (see table 4 of [17]). Simultaneously, the iron magnetic moment increases from less than $0.4\mu_B$ to more than $1.1\mu_B$ as the result of a more localized density of states. A d electron re-distribution is demonstrated convincingly by magnetization, neutron diffraction and ^{57}Fe Mössbauer spectroscopy measurements. On the P-rich side (the AF state), there results: (i) an increase in the iron band width with a reduced d moment (namely a weaker ferromagnetic character), (ii) a depletion of the density of states at the Fermi level favouring antiferromagnetic correlations, (iii) a reinforcement of the magnetocrystalline anisotropy at the tetrahedral site (as shown by the magnetization measurements and the occurrence of a sine spin wave modulation) via a spin–orbit type mechanism. The resulting long-range magnetic polarization state appears markedly field-dependent. Band structure calculations are now in progress to verify these assumptions [22].

References

[1] Fruchart R 1982 *Ann. Chimie Fr.* **7** 563
[2] Thèse Artigas M 1992 *PhD Thesis* Université de Grenoble
[3] Chenevier B 1990 *PhD Thesis* Université de Grenoble
[4] Radhakrishna P, Fujii H, Brown P J, Doniach S, Reichardt X and Schweiss P 1990 *J. Phys.: Condens. Matter* **2** 3359
[5] Fruchart R, Roger A and Sénateur J P 1969 *J. Appl. Phys.* **40** 1250
[6] Wäppling R, Häggström L, Ericsson T, Devanacayanan S, Karlsson E, Carlsson B and Rundqvist S 1975 *J. Solid State Chem.* **13** 258
[7] Eriksson O, Sjöström J, Johansson B, Häggström L and Skriver H L 1988 *J. Magn. Magn. Mater.* **74** 347
[8] Severin L, Häggström L, Nordström L, Andersson Y and Johansson B 1995 *J. Phys.: Condens. Matter* **7** 185
[9] Grandjean F, Gérard A and Sobry R 1973 *Int. J. Magn.* **4** 1
[10] Srivistava B K, Ericsson T, Häggström L, Verma H R, Andersson Y and Rundqvist S 1987 *J. Phys. C: Solid State Phys.* **20** 463
[11] Sjöström J, Häggström L and Sundqvist T 1988 *Phil. Mag.* B **57** 737

[12] Dolia S N, Krishnamurthy A, Ghose V and Srivastava B 1993 *J. Phys.: Condens. Matter* **5** 451
[13] Onnerud P, Andersson Y, Tellgren R, Ericsson T, Nordblad T, Krishnamurthy A and Srivastava B K 1995 *J. Magn. Magn. Mater.* **147** 346
[14] Eriksson O and Svane A 1989 *J. Phys.: Condens. Matter* **1** 1589
[15] Jian-Wang C, He-Lie L and Qing-Qi Z 1993 *J. Phys.: Condens. Matter* **5** 9307
[16] Zach R, Guillot M and Fruchart R 1990 *J. Magn. Magn. Mater.* **89** 221
[17] Bacmann M, Soubeyroux J L, Barrett R, Fruchart D, Zach R, Niziol S and Fruchart R 1994 *J. Magn. Magn. Mater.* **134** 59
[18] Zach R, Malaman B, Bacmann M, Fruchart R, Niziol S, Le Caër G, Soubeyroux J L, Zukrowski J and Fruchart D 1995 *J. Magn. Magn. Mater.* **147** 201
[19] Le Caër G and Dubois J M 1979 *J. Phys. E: Sci. Instrum.* **12** 1083
[20] Le Caër G and Dubiel S M 1990 *J. Magn. Magn. Mater.* **92** 251
[21] Niculescu V and Budnick J I 1978 *Solid State Commun.* **26** 607
[22] Tobola J and Karpzyk S 1996 to be published